Chinese Chemical Letters 34 (2023) 107202

Contents lists available at ScienceDirect

Chinese Chemical Letters

journal homepage: www.elsevier.com/locate/cclet

A biobased flame retardant towards improvement of flame retardancy and mechanical property of ethylene vinyl acetate

Siyi Xu[a,b,c], Yue Han[a,b,c], Cheng Zhou[b,c], Jianxi Li[b,c], Liguo Shen[a,*], Hongjun Lin[a,*]

[a] College of Geography and Environmental Sciences, Zhejiang Normal University, Jinhua 321004, China
[b] National Energy Life Evaluation and Management Technology Lab of Nuclear Power and Nonmetal Materials, Suzhou 215400, China
[c] CGN-DELTA (Taicang) Testing Technology Co., Ltd., Suzhou 215400, China

ARTICLE INFO

Article history:
Received 26 November 2021
Revised 30 December 2021
Accepted 3 February 2022
Available online 6 February 2022

Keywords:
Flame retardant
Smoke suppression
Mechanical properties
Magnesium hydroxide
Phytic acid

ABSTRACT

A new biobased flame retardant (MHPA) with remarkable compatibility was synthesized *via* a facile and low-cost neutralization reaction of magnesium hydroxide (MH) and phytic acid (PA). By blending the prepared MHPA into ethylene vinyl acetate (EVA), the fire retardancy, smoke suppression and mechanical properties of the composites were significantly improved. When 50 wt% of MH was added into EVA matrix, the value of limiting oxygen index (LOI) reached 26.1%. Whereas, when 10 wt% MH in the EVA composites (with initial 50 wt% MH) was replaced by MHPA, the resulted EVA composites had a LOI value of 30.8%, indicating high efficiency of addition of MHPA to improve flame retardancy. Moreover, the heat release rate (HRR) and total smoke production (TSP) of the EVA composites reduced by 54.4% and 27.6%, respectively, suggesting that incorporation of MHPA could effectively hinder rapid degradation of EVA composites during burning process. The fire-retardant mechanism may reside in that the MHPA combined with MH can present the excellent carbonization and expansion effects. This study illustrates that the biobased MHPA has a broad application prospect to develop flame-retardant EVA composites.

© 2022 Published by Elsevier B.V. on behalf of Chinese Chemical Society and Institute of Materia Medica, Chinese Academy of Medical Sciences.

Ethylene vinyl acetate copolymer (EVA) materials have been widely applied in various areas such as hot melt adhesive [1], cable insulation pipe [2], automobile [3] and coating [4] due to their great flexibility, shockproof, skid and strong pressure resistance [4,5]. However, the high flammability of EVA extremely restrains the applications due to the fact that numerous and noxious smokes generated from EVA would greatly threaten the life safety of people during the process of fire escape [6]. Therefore, extensive efforts have been devoted to improving the smoke suppression and flame retardancy properties of EVA [7,8].

Halogen flame retardants including chlorine and bromine elements can efficiently promote the flame-retardant ability of EVA. However, they are considered to be controversial flame retardants because that they release a lot of toxic smokes during the combustion process [9]. With the growing concern on environmental problems in recent years, the halogen free magnesium hydroxide (MH) has received increasing attention in the flame-retardant area. MH, as one of the metal hydrate flame retardants, possesses many advantages including halogen free, smoke suppression, innocuity and low cost. It has been extensively used as the environmental-friendly flame-retardant for EVA composites. However, MH is found to have drawbacks such as poor compatibility and low efficiency, negatively effect on processability and mechanical properties [10–12]. To overcome the defects of single flame retardant, synergistic flame retardants have recently become an important research direction because of their obvious superiority. Coordinating with other flame retardants, such as ammonium polyphosphate [13] and expanded graphite [14,15], MH can display effective synergetic flame retardancy. However, poor mechanical properties and high-cost issues are still the primary obstacle for the industrial applications. In order to conquer these difficulties, surface functionalization such as grafting and modification has been developed as an uncomplicated and highly efficient method. For instance, MH nanoparticles have been successfully grafted by 9,10-dihydro-9-oxa-10-phosphaphenanthr-ene-10-oxide (DOPO) to achieve the excellent mechanical and processing properties of the EVA composites [16]. Moreover, the modification of triethoxysilane and polymethyl-vinyl silicone rubber can greatly improve the interfacial compatibility between MH flame retardant and PP matrix [17]. As a typical biomass-derived phosphoric acid, phytic acid (PA) is generally derived from beans and cereal grains in nature. PA with 28 wt% of phosphorus can be regarded as the acid source for dehydration [18,19], which has become a potential flame retardant because of its excellent carbonization ability. In addition,

* Corresponding authors.
E-mail addresses: lgshen@zjnu.cn (L. Shen), hjlin@zjnu.cn (H. Lin).

https://doi.org/10.1016/j.cclet.2022.02.008
1001-8417/© 2022 Published by Elsevier B.V. on behalf of Chinese Chemical Society and Institute of Materia Medica, Chinese Academy of Medical Sciences.

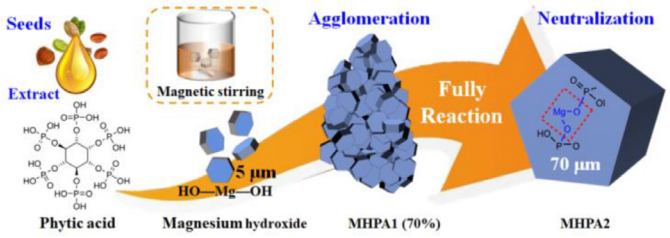


Fig. 1. Synthetic route of MHAP synergistic flame retardant.

the cyclohexane from PA is also an important carbon source, which means PA itself can generate certain char residue *via* the simultaneous dehydration and carbonization during combustion process. However, due to its strong acidity and poor thermal stability, it is hardly possible to directly use PA as a flame retardant. A potential solution for this limitation is to develop a synergistic flame retardant *via* chemical reaction. For example, the melamine [20], piperazine [21] and UiO-66-NH_2 [22] can chemically react with PA to produce the complex compounds with phosphorous-nitrogen synergistic flame retardant effect [23]. Inspired from the above studies, it is hypothesized that combination of PA and MH *via* chemical reactions would give out a synergistic flame retardant. However, to our knowledge, no literature work has been carried out to test this hypothesis.

In current work, a new biobased flame retardant (MHPA) was firstly developed by a facile and low-cost chemical reaction between PA and MH to synergistically improve mechanical properties and flame retardancy of EVA composites. The structure, morphology and thermal stability of the biobased flame retardant were characterized by Fourier transform infrared spectroscopy (FTIR), scanning electron microscopy (SEM), X-ray photoelectron spectroscopy (XPS) and thermogravimetric analyzer (TGA). Thereafter, the EVA composites with MHPA were evaluated in terms of fire retardancy, thermal stability and mechanical properties. In addition, the residues of these composites after burning were investigated to illustrate the possible flame-retardant mechanism of MHPA.

The following materials were used in this experiment. EVA 2803 (28% vinyl acetate; molecular weight: 114.143; melting point: 99 °C; boiling point: 170.6 °C; density: 0.92–0.98 g/cm^3) was brought from Arkema (France). Phytic acid (concentration: 70 wt%; molecular weight: 660.04; boiling point: 105 °C; density: 2.42 g/cm^3) was purchased from Shanghai Zhanyun Chemical Co., Ltd. MH 5P-C (specific surface area: 3–10 m^2/g; average particle size: 1–10 μm; density: 2.36 g/cm^3) was offered by Kyowa Chemical industry Co., Ltd.

The synthetic route of the MHPA synergistic flame retardant is shown in Fig. 1. Firstly, 100 mL DI water was used to dissolve 5.00 g MH to form a uniform suspension by stirring the mixture for 5 min. Secondly, 13.3 ml PA solution (70 wt%) was slowly dropped into the suspension with a continuous stirring for 5 min. Then, these obtained bulk products marked as "MHPA1 (70%)" were washed and then dried at 60 °C for 48 h. Thereafter, the MHPA1 (70%) was sieved (200 mesh) to obtain uniform particle powders. The MHPA1 (70%) was further reacted with 6 ml PA solution (30 wt%) *via* the same procedure in the previous step, and the resultant products were marked as "MHPA2". To check whether the reaction was completed, the PA solution (30 wt%) was used to react with MHPA2 again to obtain the resultant products marked as "MHPA3" *via* the same method mentioned above.

The composition of EVA/MH/MHPA composites is listed in Table S1 (Supporting information). The materials were homogeneously blended at 85 °C for 10 min by a two-roll mill, and then molded by hot pressing (175 °C, 10 MPa) for 8 min. Thereafter, these obtained

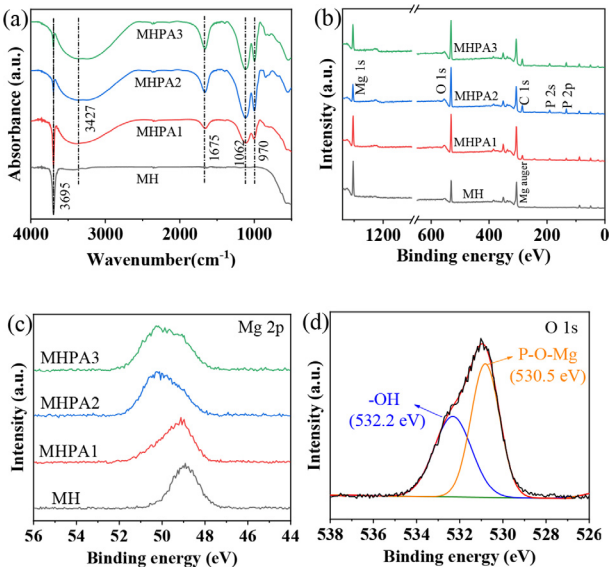


Fig. 2. Characterization profiles of prepared samples: (a) FTIR spectra; (b) XPS survey; (c) XPS spectra of Mg 2p; (d) XPS spectra of O 1s of MHPA2.

sheets were sliced into specimens with suitable sizes for different tests.

The prepared samples were investigated by scanning electron microscopy (SEM, Phenom ProX, Phenom, China) [24–26], energy dispersive spectrometer (EDS, Phenom ProX, Phenom, China), Fourier-transform infrared spectroscopy (FTIR, TENSOR27, Bruker, Germany) [27,28], X-ray photoelectron spectroscopy [29–31] (XPS, Escalab 250Xi, Thermo Fisher Scientific, USA), and thermogravimetric analyzer (TGA, Q50, TA, USA). Limit oxygen index (LOI, JF-3, Zhengrui Taibang Co., Ltd, China) and cone calorimeter (CONE, CCT, MOTIS, China, with 50 kW/m^2 heat flux) measurements was carried out to assess the flame retardancy of the samples. The residues collected from cone calorimeter tests were evaluated by SEM, FTIR and Raman spectra (RS, ATR 3110–1064, OPTOSKY, China). The thermal degradation of EVA and its composites was obtained by TGA (N_2, 20 °C/min, 50–800 °C). The mechanical properties were obtained by using a universal testing machine (Rate: 250 mm/min; UTM4204, SUNS, China), and the brittle sections were observed by SEM.

The characterization profiles of MH, MHPA1, MHPA2 and MHPA3 are presented in Fig. 2. As shown in FTIR spectra (Fig. 2a), the characteristic sharp peak at 3695 cm^{-1} is due to O–H stretching vibration of MH. MHPA1 presents a relative lower intensity peak of O–H, which is due to that the reaction between MH and PA consumes part of O–H [32]. The decreasing intensity of 3695 cm^{-1} indicates that more and more O–H has been consumed by the reaction between MH and PA. Furthermore, the wide absorption peaks ranged from 3550 cm^{-1} to 3200 cm^{-1} are attributed to the hydrogen bonds and the stretching vibration of P–OH [33], which indicates the connection between MH and PA is dominated by hydrogen bonds. Meanwhile, the new characteristic absorption peaks at 1675 cm^{-1} (O–H bending vibration), 1062 cm^{-1} (P–O stretching vibration) and 970 cm^{-1} (P–O–C stretching vibration) indicate existence of PA [34]. In Fig. 2b, the characteristic peaks including Mg 1s (1298 eV) and O 1s (532.1 eV) can be observed in all samples [35]. In addition, three additional peaks at 133.5, 191.1 and 285.1 eV can be attributed to the P 2p, P 2s and C 1s orbitals, respectively. The intensity of these peaks of MHPA1 are much weaker than those of MHPA2 and MHPA3 as a result of incomplete reaction between MH and PA. In Fig. 2c, the Mg 1s (49.5 eV) peak moves to higher binding energy direction owing to the effect of

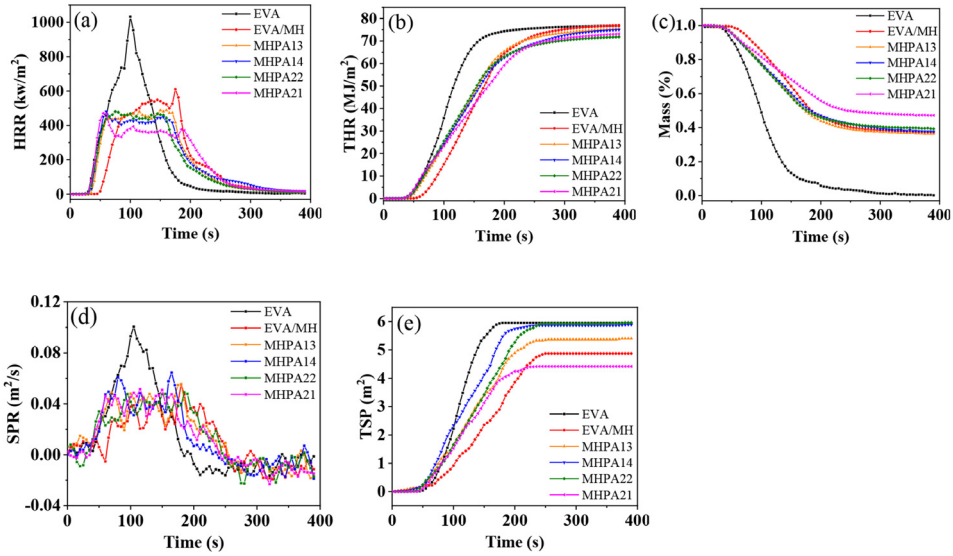


Fig. 3. HRR (a), THR (b), Mass (c), SPR (d) and TSP (e) curves of samples.

neutralization reaction between the MH and PA. Moreover, two mixed O 1s peaks (532.2 and 530.5 eV) in Fig. 2d confirm the formation of fresh Mg–O–P bonds in the MHPA samples [36]. As all, FTIR spectra clearly demonstrate the reaction between MH and PA.

The SEM images in Fig. S1 (Supporting information) display the morphologies and EDS results of MHPA samples. It is found that the MHPA1 shows a loose structure and with 2.77% of P content, which manifests the incomplete neutralization reaction between MH and PA. While the MHPA2 presents a compact and dense caking structure (Fig. S1b) when the neutralization reaction takes place sufficiently. The increased P content (11.13%) also indicates the completed neutralization reaction. Furthermore, it seems that more reactants (PA) cannot significantly change the MHPA structure and P content, as shown in Fig. S1c.

LOI tests of the EVA composites were conducted, and the results are summarized in Table S1. The LOI value of pristine EVA is only 18% that may lead to numerous security risks as a result of extremely flammability [37]. When 50 wt% of MH is added into EVA matrix, the value of LOI increases to 26.1%. Although the apparent improvement achieved compared with pure EVA, the EVA/MH composite still belongs to a kind of combustible materials according to identification standard [38]. When MHPA compositions are introduced into EVA/MH composites, it is interestingly found that the LOI value can be significantly promoted and even reaches to 30.8%. This indicates that MHPA has the excellent performance in obstructing ignition and burning.

The cone calorimeter tests are performed to discuss the combustion behavior of EVA composites, and the results are presented in Fig. 3 and Table S2 (Supporting information). The ignition time (TTI) of neat EVA is 38 s and the TTI extends when the flame retardant is added. Among EVA composites, the TTI of EVA/MH composite is improved to 58 s owing to the constant heat absorption effect of MH, while those of MHPA13, MHPA14, MHPA22 and MHPA21 are reduced to 44 s, 45 s, 43 s and 44 s, respectively, which should be put down to the thermal decomposition of the MHPA1 and MHPA2. Fig. 3a shows that pure EVA rapidly burns with single sharp peak, and the heat release rate (HRR) peak value is 1032.1 kW/m^2. While EVA/MH composite displays a continuously raising curve of HRR and the steep peak appears at 180 s with the value of HRR of 610.4 kW/m^2. The HRR curves of MHPA13, MHPA14 and MHPA22 indicate the similar broad platform between 55 s and 160 s, which means the incorporation of MHPA could effectively change the degradation process and hinder the rapid degradation of EVA composites during burning process [35]. This result suggested the good synergistic effect between MH and MHPA which prevents fire and oxygen transmission and suppress the violent degradation and combustion of the underlying matrix [39]. Furthermore, Fig. 3b exhibits that the samples' total heat release (THR) is obviously delayed by incorporating MHPA flame retardants, which effectively limits the speed of heat generation [22]. Fig. 3c shows the mass curves of the EVA composites. Almost no residue of pure EVA could be found after burning due to the complete decomposition, in line with the previous report [40]. With the incorporation of these flame retardants, the residual yields of the EVA composites are hugely increased. It is worth noting that the char residual yield of MHPA21 reaches to 46.6% (the highest value) as a result of the synergism from dehydration and carbonization of phosphorus and carbon compounds produced by MHPA and the endothermic effect of MH [21]. The total smoke production (TSP) and smoke production rate (SPR) curves in Figs. 3d and e indicate that the release of smoke is restrained in the early stage of combustion. MHPA21 generates the lowest smoke (4.3 m^2), which could be mainly put down to the excellent barrier effect of char residue formed by MHPA and MH.

The TGA and DTG profiles of EVA and EVA composites are exhibited in Fig. S2 (Supporting information) and the relative data are shown in Table S3 (Supporting information). The $T_{5\%}$ of EVA is promoted from 340.8 °C to 354.7 °C when the MH is added in. Moreover, the addition of MHPA does not significantly reduce the thermal stability of their composites, indicating the synergistic effect of MH and MHPA [41].

Fig. 4 exhibits the digital photos of the char residues after cone calorimeter test for EVA and its composites. There is not residue formed in Fig. 4a because of the poor carbonaceous property of EVA. The residues of EVA composites could be observed, as shown in Figs. 4b-f. The homogeneous char residue (Fig. 4f) of MHPA21 implies that the incorporation of MHPA2 could generate superior synergism with MH and form high quality char yield to isolate flammable gasses and heat, hence protect the EVA composite from being ignited in a short time [42]. Furthermore, the expansion effects of MHPA22 and MHPA21 are displayed by the side digital photos in Figs. 4g and h. The carbonized layer of MHPA22 is rugged with serious cracks, which makes it difficult to isolate the heat and fire. While the carbonized MHPA21 is in a smooth and intact char

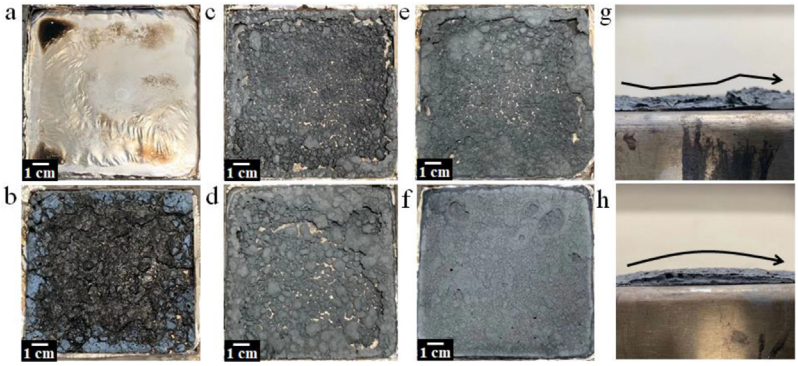


Fig. 4. Digital images of char residues after combustion: (a) pure EVA, (b) EVA/MH, (c) MHPA13, (d) MHPA14, (e) MHPA22, and (f) MHPA21. The side digital photos of MHPA22 (g) and MHPA21 (h).

layer with an excellent expansion effect [43]. And the micro characteristics are further analyzed in Figs. S3a-e (Supporting information) by SEM analysis. As shown in Fig. S3a, lots of holes can be found on the char surface of EVA/MH composite due to the release of excessive water volatilization from MH. Meanwhile, several cracks and flaws could be perceived in Figs. S3b-d. Whereas, the MHPA21 sample (Fig. S3e) gave no holes and cracks. Since both holes and cracks would destroy the flame retardancy, MHPA21 sample possesses the optimal flame retardancy ability due to the prominent synergism between MHPA2 and MH.

The structure stability of these char residues was analyzed by Raman spectroscopy, and the results are shown in Fig. S4 (Supporting information). The strong peaks discovered at 1310 and 1600 cm^{-1} are signed to the D and G peaks, respectively. The D-peak and G-peak represent the defect of C-atom lattice and the in-plane stretching vibration of C-atom sp^2 hybrid, respectively [44]. The intensity rate (I_D/I_G) of the D-peak to G-peak reveals the degree of graphitization. The lower of I_D/I_G value is, the higher the degree of graphitization and the dense of char residue are [44]. From Figs. S4a-e, the I_D/I_G values of EVA/MH, MHPA13, MHPA14, MHPA22 and MHPA21 composites are 0.68, 0.57, 0.51, 0.51 and 0.42, respectively. MHPA21 displays the lowest I_D/I_G value, indicating the dense char residue and the highest graphitization degree. Additionally, the char residue of EVA composites is also analyzed, as shown in Fig. S4f. The residues of EVA/MH composite display only a characteristic peak at 500 cm^{-1} (Mg–O), which means the residue is magnesium oxide. Whereas, MHPA samples show more signals due to in-plane and out-of-plane bending of C–O–H at 1435 and 940 cm^{-1}, the C–O stretching vibration of P–O–C at 1060 cm^{-1} and the symmetric vibration of P–O in P–O–P at 1000 cm^{-1}. Furthermore, it is evident to notice that the MHPA21 gives out a fresh single peak of 3452 cm^{-1}, which might be the valence vibration of O–H in P–OH [45,46]. It could be interpreted that P–OH is not completely consumed during combustion due to the protection of external char yield [47], which makes a further contribution of synergistic flame retardancy.

Apart from the essential flame retardancy, mechanical properties are also equivalently important to EVA composites in various fields. As shown in Fig. S5 (Supporting information), the tensile strength of EVA/MH composite seriously decreases and the elongation is reduced to 220%, which could be interpreted by the poor organic and inorganic compatibility between EVA and MH. When the MHPA is added into EVA, the elongation of EVA composites reaches 525% which is 2.38 times higher than that of EVA/MH composite.

Pure EVA could not generate any char layer to block fire and heat, which is a potential fire hazard in applications. After incorporation of MHPA, the combustion process is significantly changed, as shown in Fig. S6 (Supporting information). On the one hand, the phosphoric acid and metaphosphoric acid and even polymetaphosphoric acid are generated by dehydration and carbonization during combustion process [48]. In this process, an impact char layer is formed and can isolate flammable gasses and fire and produce a strong flame-retardant effect [34]. On the other hand, the MHPA2 plays a role of capturing free radicals. During combustion process, the $PO^{\bullet -}$, $HPO^{\bullet -}$ and HPO_2 produced from MHPA could capture the external $^{\bullet}OH$ and $H^{\bullet}$ radicals to weaken the degradation of main chains of EVA [48]. In addition, MH releases vapors and forms MgO to strength the compactness of char layer which further suppresses the spread of fire [49].

A novel biobased MHPA flame retardant is successfully synthesized by neutralization reaction between MH and PA. When 10 wt% MH in EVA composites (with 50 wt% MH) was replaced by MHPA, the LOI value increased to 30.8% while that of pure EVA was only 18%. In addition, MHPA could give out dense char residues during combustion, which also contributed to the flame retardancy. Moreover, the addition of MHPA acts as a compatibilizer who remarkably promotes the elongation at break of EVA/MH composite to 525%. Since the biobased flame retardant can endow excellent property to EVA composites, which are able to possess broad application prospects, such as aerospace industry, nuclear power industry *etc.*

Declaration of competing interest

The authors declare that they have no known competing financial interests or personal relationships that could have appeared to influence the work reported in this paper.

Acknowledgments

Financial support of Zhejiang Outstanding Youth Fund (No. LR22E080007), National Natural Science Foundation of China (Nos. 52070170, 51978628) and Zhejiang Provincial Ten Thousand Talent Program (No. ZJWR0302055) are highly appreciated.

Supplementary materials

Supplementary material associated with this article can be found, in the online version, at doi:10.1016/j.cclet.2022.02.008.

References

[1] H.H. Chu, W.H. Huang, K.S. Chuang, B.H. Shen, Int. J. Adhes. Adhes. 99 (2020) 102586.
[2] M. Sabet, A. Hassan, C.T. Ratnam, Polym. Degrad. Stabil. 97 (2012) 1432–1437.
[3] S. Ramarad, C.T. Ratnam, M. Khalid, A.L. Chuah, S. Hanson, Radiat. Phys. Chem. 130 (2017) 362–370.
[4] S.P. Tambe, S.K. Singh, M. Patri, D. Kumar, Prog. Org. Coat. 62 (2008) 382–386.

[5] M.C. Carvalho de Oliveira, A.S. Alves Cardoso Diniz, M.M. Viana, V.d.F. Cunha Lins, Renewable Sustainable Energy Rev. 81 (2018) 2299–2317.
[6] F.E. Ngohang, G. Fontaine, L. Gay, S. Bourbigot, Polym. Degrad. Stab. 115 (2015) 89–109.
[7] L. Shen, C. Shao, R. Li, et al., Polym. Bull. 76 (2019) 2399–2410.
[8] G. Yu, Y. Liu, J. Li, Polym. Adv. Technol. 29 (2018) 1804–1814.
[9] J.M. Allgood, T. Jimah, C.M. McClaskey, et al., Environ. Res. 153 (2017) 55–62.
[10] Y. Gao, J. Wu, Q. Wang, C.A. Wilkie, D. O'Hare, J. Mater. Chem. A 2 (2014) 10996–11016.
[11] F. Laoutid, L. Bonnaud, M. Alexandre, J.M. Lopez-Cuesta, P. Dubois, Mat. Sci. Eng. R: Rep. 63 (2009) 100–125.
[12] L. Ye, Q. Wu, B. Qu, Polym. Degrad. Stab. 94 (2009) 751–756.
[13] F. Lou, K. Wu, Q. Wang, et al., Polymers-Basel 11 (2019) 125.
[14] Y. Liu, L. Shen, Z. Huang, et al., J. Membr. Sci. 641 (2022) 119925.
[15] X. Wu, L. Wang, C. Wu, G. Wang, P. Jiang, J. Appl. Polym. Sci. 126 (2012) 1917–1928.
[16] T. Liu, F. Wang, G. Li, et al., J. Appl. Polym. Sci. 138 (2021) 49607.
[17] L. Liu, M. Xu, Y. Hu, et al., J. Appl. Polym. Sci. 136 (2019) 47129.
[18] X.W. Cheng, J.P. Guan, R.C. Tang, K.Q. Liu, J. Cleaner Prod. 124 (2016) 114–119.
[19] W. Zhu, S. Hao, M. Yang, B. Cheng, J. Zhang, Cellulose (2020) 1–12.
[20] Z. Zheng, S. Liu, B. Wang, et al., Polym. Compos. 36 (2015) 1606–1619.
[21] Y.Y. Gao, C. Deng, Y.Y. Du, S.C. Huang, Y.Z. Wang, Polym. Degrad. Stab. 161 (2019) 298–308.
[22] J. Zhang, Z. Li, L. Zhang, Y. Yang, D.Y. Wang, ACS Sustain. Chem. Eng. 8 (2020) 994–1003.
[23] L. Wang, J. Zhan, L. Song, Y. Hu, R.K.K. Yuen, J. Appl. Polym. Sci. 131 (2014) 40112.
[24] M. Wu, Y. Chen, H. Lin, et al., Water Res. 181 (2020) 115932.
[25] S. Xu, J. Li, Q. Ye, L. Shen, H. Lin, J. Colloid Interface Sci. 589 (2021) 525–531.
[26] K. Shang, W. Liao, Y.Z. Wang, Chin. Chem. Lett. 29 (2018) 433–436.
[27] Y. Long, G. Yu, L. Dong, et al., Water Res. 189 (2020) 116665.
[28] T. Sun, Y. Liu, L. Shen, et al., J. Colloid Interface Sci. 570 (2020) 273–285.
[29] Y. Xu, Y. Xiao, W. Zhang, et al., J. Membr. Sci. 618 (2021) 118726.
[30] Q. Zeng, Y. Liu, L. Shen, et al., J. Colloid Interface Sci. 582 (2021) 291–300.
[31] Z. Huang, J. Liu, Y. Liu, et al., J. Membr. Sci. 623 (2021) 119080.
[32] D. Yao, G. Yin, Q. Bi, et al., Polymers-Basel 12 (2020) 2107.
[33] S. Xu, Q. Gao, C. Zhou, et al., Mater. Chem. Phys. 274 (2021) 125182.
[34] W.X. Li, H.J. Zhang, X.P. Hu, et al., J. Hazard. Mater. 398 (2020) 123001.
[35] B. Chen, H. Xie, L. Shen, et al., J. Membr. Sci. 640 (2021) 119820.
[36] W. Meng, W. Wu, W. Zhang, et al., Poly. Int. 68 (2019) 1759–1766.
[37] B. Wang, X. Qian, Y. Shi, et al., Compos. Part B: Eng. 69 (2015) 22–30.
[38] Y.Y. Yen, H.T. Wang, W.J. Guo, Polym. Degrad. Stab. 97 (2012) 863–869.
[39] Z. Huang, Q. Zeng, Y. Liu, et al., J. Membr. Sci. 640 (2021) 119854.
[40] Y. Wang, X. Yang, H. Peng, et al., ACS Appl. Mater. Interfaces 8 (2016) 9925–9935.
[41] L.F. Fang, B.K. Zhu, L.P. Zhu, H. Matsuyama, S. Zhao, J. Membr. Sci. 524 (2017) 235–244.
[42] Y. Liu, Q. Yu, Z. Fang, Y. Zhang, Polym. Polym. Compos. 23 (2015) 345–350.
[43] F. Zhang, W. Sun, Y. Wang, B. Liu, J. Appl. Polym. Sci. 132 (2015) 42148.
[44] W. Guo, S. Nie, E.N. Kalali, et al., Compos. Part B: Eng. 176 (2019) 107261.
[45] R. Chen, Z. Luo, X. Yu, et al., Carbohyd. Polym. 245 (2020) 116530.
[46] N. Zhang, J. Zhang, H. Yan, et al., J. Hazard. Mater. 373 (2019) 856–865.
[47] X. Hu, X. Zhu, Z. Sun, Constr. Build. Mater. 256 (2020) 119445.
[48] D. Wang, Y. Wang, T. Li, et al., ACS Sustain. Chem. Eng. 8 (2020) 10265–10274.
[49] Y. Pan, Z. Luo, B. Wang, J. Appl. Polym. Sci. 138 (2021) 49813.